Materials Letters 83 (2012) 27–30

Contents lists available at SciVerse ScienceDirect

Materials Letters

journal homepage: www.elsevier.com/locate/matlet

Graphene-encapsulated $LiFePO_4$ nanoparticles with high electrochemical performance for lithium ion batteries

Huan Xu, Jie Chang, Jing Sun *, Lian Gao

The State Key Laboratory of High Performance Ceramics and Superfine Microstructures, Shanghai Institute of Ceramics, Chinese Academy of Sciences, 1295 Dingxi Road, Shanghai 200050, PR China

ARTICLE INFO

Article history:
Received 8 March 2012
Accepted 28 May 2012
Available online 1 June 2012

Keywords:
Nanocomposites
Surfaces
Structural
Energy storage and conversion

ABSTRACT

Graphene-encapsulated $LiFePO_4$ nanospheres have been developed by a solid state reaction using the graphene oxide-encapsulated FeOOH as raw materials. The $LiFePO_4$ nanospheres with an average diameter of ~20 nm were wrapped tightly with a 3D graphene network. Such a special nanostructure facilitated the electron and lithium ion migration to provide good electrochemical performance, especially at high current rates. This graphene-encapsulated $LiFePO_4$ material could deliver discharge capacities of 166.6, 108.6 and 90.6 mAh g^{-1} at 0.1 C, 5 C and 10 C respectively and showed a capacity decay of <9% when cycled 5 C and 10 C charge/discharge for 300 times.

1. Introduction

Olivine-structured $LiFePO_4$ (LFP) is one of the most promising cathode materials for lithium ion batteries, because of its nontoxicity, safety, high capacity, long cycle life, thermal stability and low-cost [1–3]. However the low electronic conductivity and slow lithium ion diffusion rate constrain the electrochemical performance, especially the high-rate performance. Numerous attempts have been made to solve these problems, such as particle size reduction [4], carbon coating [5,6] and aliovalent doping [7].

Graphene with a two-dimensional monolayer sheet of sp^2-bonded carbon atoms has large specific surface area (2630 m^2 g^{-1}), excellent electrical conductivity, good mechanical flexibility and strong thermal/chemical stability. The incorporation of graphene into the compound materials as a reinforcing component can provide them with the unique functions of graphene. Hereby a lot of graphene modified materials with enhanced performance are investigated and applied in different fields such as sensors, catalysis, supercapacitors, hydrogen storage and lithium ion batteries [8–11]. Hitherto, graphene modified materials as anodes and cathodes for rechargeable lithium-ion batteries have been intensive explored. Ji et al. demonstrated that graphene modified Fe_3O_4 exhibited much better electrochemical performance than pure Fe_3O_4 nanoparticles [12]. At the same time, graphene modified Sn was proved improved electrochemical performance compared with pure graphene and Sn [13]. Garphene was used to buffer the huge volume change of the active materials, preserve the electrode integrity upon continuous charge/discharge cycles, and enable efficient ion and electron transport. But, the active material particles just intersperse on graphene, and these particles partially contact graphene, resulting in a limited enhancement in electron conductivity. Yang et al. [14] confirmed that the graphene-encapsulated Co_3O_4 exhibited better discharge performance and cycle stability than mechanical mixture of graphene and Co_3O_4 because of lower contact and charge-transfer impedances. Since the graphene-encapsulated structure can improve the electron conductivity much better, which can ameliorate low electronic conductivity, one of the disadvantages of $LiFePO_4$ material, such a special structure applied to $LiFePO_4$ material can enhance the electrochemical performance a lot. Herein, we synthesize graphene oxide-encapsulated FeOOH nanopartilces(GOE-FeOOH) first and successfully transform them to graphene-encapsulated $LiFePO_4$ nanospheres (GE-LFP) through solid state reaction. GE-LFP showed excellent rate capability and cycle stability.

2. Experimental details

All chemicals were of analytical grade and used as received. GO was made from natural graphite via a modified Hummers method [15]. FeOOH nanoparticles were prepared by the hydrolysis of aqueous $FeCl_3$ solution [16]. 0.5 g of FeOOH nanoparticles was dispersed into 50 mL toluene via sonication. After 2 h, 0.5 mL of aminopropyltrimethoxysilane (APS) was added into the above solution and refluxed for 24 h under argon atmosphere to obtain APS-modified FeOOH. Then 400 mL APS-modified FeOOH dispersion (0.25 mg mL^{-1}) was added into 400 mL aqueous GO suspension (0.05 mg mL^{-1}) under mild magnetic stirring. After 1.5 h, the above suspension was filtered and dried at 60 °C to obtain GOE-FeOOH. The final GE-LFP composite was prepared by a solid state

* Corresponding author. Tel.: +86 21 52414301; fax: +86 21 52414903.
E-mail address: jingsun@mail.sic.ac.cn (J. Sun).

0167-577X/$ – see front matter © 2012 Elsevier B.V. All rights reserved.
doi:10.1016/j.matlet.2012.05.116

reaction. The mixture of GOE-FeOOH, $LiCH_3COO \cdot 2H_2O$, $NH_4H_2PO_4$ (in molar ratio = 1:1:1) and polyethylene glycol (PEG-4000, 100 mg PEG per 1 mmol LFP) was milled with ethanol for 20 h. The dried mixture was heated at 300 °C for 2 h and 700 °C for 10 h respectively with a heating rate of 10 °C/min to get the final product GE-LFP. Here, polyethylene glycol was used to further coat $LiFePO_4$ with carbon.

Powder X-ray diffraction (XRD) patterns were recorded on a Rigaku D/MAX-2250V diffractometer using Cu Ka radiation (40 kV and 40 mA). Thermogravimetric analysis was performed on the STA 449C system (Netzsch, Germany). Field-emission scanning electron microscope (FE-SEM) was performed on Hitachi S-4800. Transmission electron microscopy (TEM) and high resolution TEM (HRTEM) images were performed on a JEOL (JEM-2100 F) microscope with an accelerating voltage at 200 kV.

Electrochemical testing was performed using coin type cells with lithium metal as the counter electrode, Celgard 2500 as the separator and 1 M $LiPF_6$ in ethylene carbonate and diethyl carbonate (EC/DMC, 1:1, w/w) as electrolyte. The working electrode was fabricated by mixing GE-LFP, acetylene black, and polyvinylidene fluoride (PVDF) with a weight ratio of 80:10:10. Cell assembly was carried out in a glove box filled with highly pure argon gas. The galvanostatic charge/discharge experiments were performed between 2 and 4.2 V at different current loads by a CT2001 battery tester.

3. Results and discussion

FeOOH nanoparticles (JCPDS Card No. 34-1266) were prepared by the hydrolysis of aqueous $FeCl_3$ solution as shown in Fig. 1a. Scanning electron microscopy (SEM) image (Fig. 1b) shows that these FeOOH nanoparticles consist of major spindle-shaped particles and minor spindle-shaped multipods with 50–100 nm in width and several hundreds of nanometers in length. The typical SEM image (Fig. 1c) of GOE-FeOOH reveals that GO sheets wrap tightly around the surface of FeOOH nanoparticles. Thermogravimetric analysis (TGA) of GOE-FeOOH reveals that the weight fraction of FeOOH in the composite is as high as 75.6%.

The XRD pattern of GE-LFP in Fig. 2f illustrates the pure orthorhombic phase of LFP (JCPDS Card No. 40-1499). LFP nanospheres with an average diameter of ~20 nm are wrapped densely by graphene huddling to a 3D continuous conductive network (Fig. 2a). The HRTEM images of regions 1 and 2 marked by white rectangles in Fig. 2a are shown in Figs. 3b and 2c. The measured fringe spacing values in Fig. 2b are 0.258 and 0.158 nm, corresponding to $(2\bar{2}0)$ and (340) planes of orthorhombic phase. The inset in Fig. 2b shows the corresponding Fast-Fourier-Transform (FFT) pattern, presenting a single-crystalline pattern with sharp diffraction spots. It can be seen that one grain (marked by black dotted curves) partially overlaps other grains in Fig. 2c. We select region 3 and 4 by black rectangles representing the non-overlapping and overlapping regions. The ordered lattice fringes in region 3 and their corresponding FFT pattern (Fig. 2d) reveal that the grain is single crystal. The interplane distances of 0.349, 0.295 and 0.231 nm can be found, corresponding to $(1\bar{1}1)$, (121) and (012) planes of orthorhombic $LiFePO_4$. However there are several diffraction patterns in region 4, consisting with the phenomenon of the overlapping grains. Carbon coating is marked in the HRTEM images as well and the carbon content in GE-LFP of 12.6 wt.% determined by TG curve (Fig. 2g) is calculated as the reported paper [17].

Electrochemical testing of GE-LFP was carried out and the capacities are calculated based on the mass of LFP with the amount of carbon being subtracted. The typical voltage-capacity curves and the specific capacities at different current rates are shown in Fig. 3a and b respectively. At the rate of 0.1 C (17 mA/g), GE-LFP delivers a discharge capacity of 166.6 mAh g^{-1}, corresponding to 98% of the theoretical capacity of $LiFePO_4$. The discharge capacities of GE-LFP reach 108.6 and 90.6 mAh g^{-1} for 5 and 10 C respectively. The cycling capability of GE-LFP at 5 and 10 C is shown in Fig. 3c and d respectively. In the 300 cycle the capacity losses are only 2.77% and 8.30% respectively. The coulombic efficiency also shown in Fig. 3c and d stays at about 100%. Besides, we investigated the morphology of GE-LFP after 50 cycles at 5 C (Inset of Fig. 3c), which almost did not change. Hereby the excellent cycle stability under fast charge/discharge conditions can mainly be ascribed to the peculiar graphene-encapsulated structure. The nanosized LFP spheres provide shorter diffusion path and graphene increases the electronic conductivity effectively. At the same time, the intimate contact between graphene and LFP nanospheres enhances the electronic conductivity and the 3D continuous graphene sheet serves as the fast path for electron migration during the charge/discharge process.

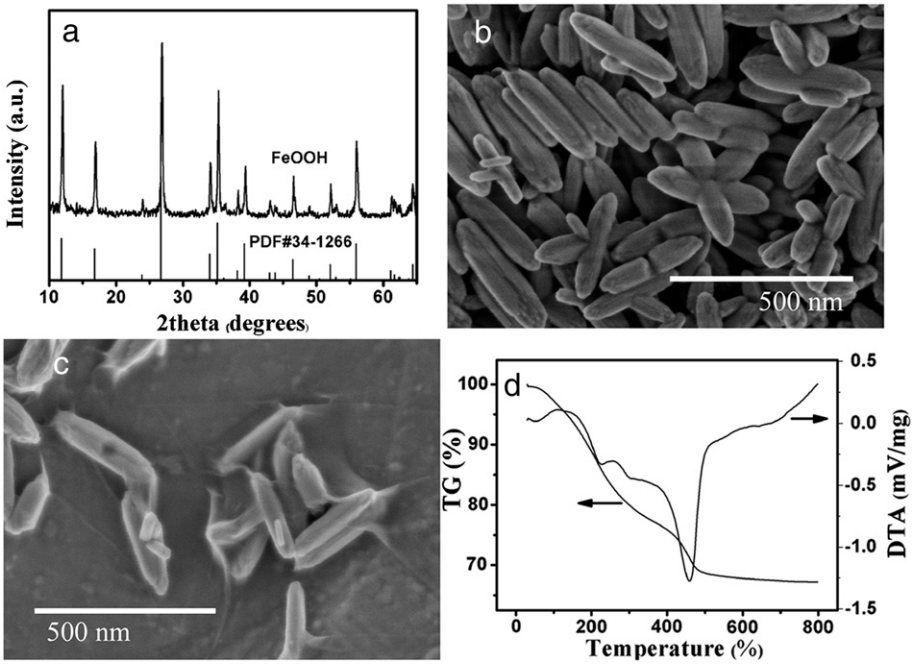

Fig. 1. (a) XRD pattern and (b) SEM image of FeOOH nanoparticles; (c) SEM image and (d) TG/DTA curves of GOE-FeOOH.

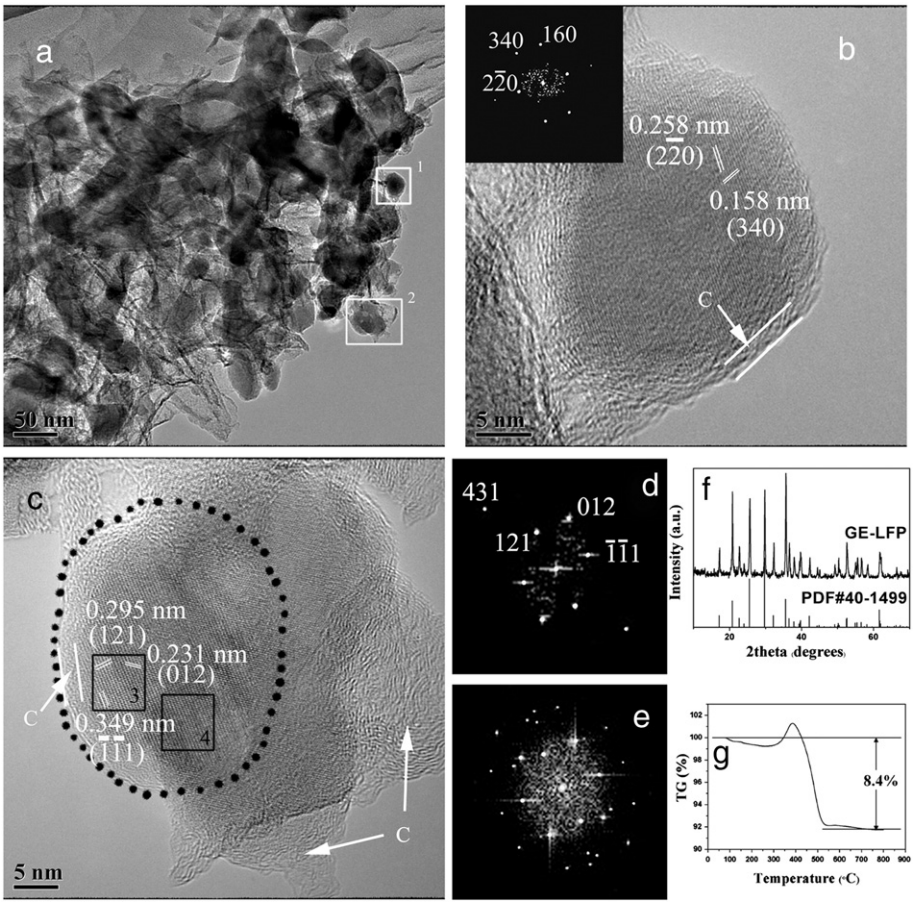

Fig. 2. Characterization of GE-LFP: (a) TEM image; (b) and (c) HRTEM images of regions 1 and 2 marked by white rectangles in (a); (d) and (e) the corresponding Fast-Fourier-Transform (FFT) images of regions 3 and 4 marked by black rectangles in (c); (d) XRD pattern and (h) TG curves of GE-LFP.

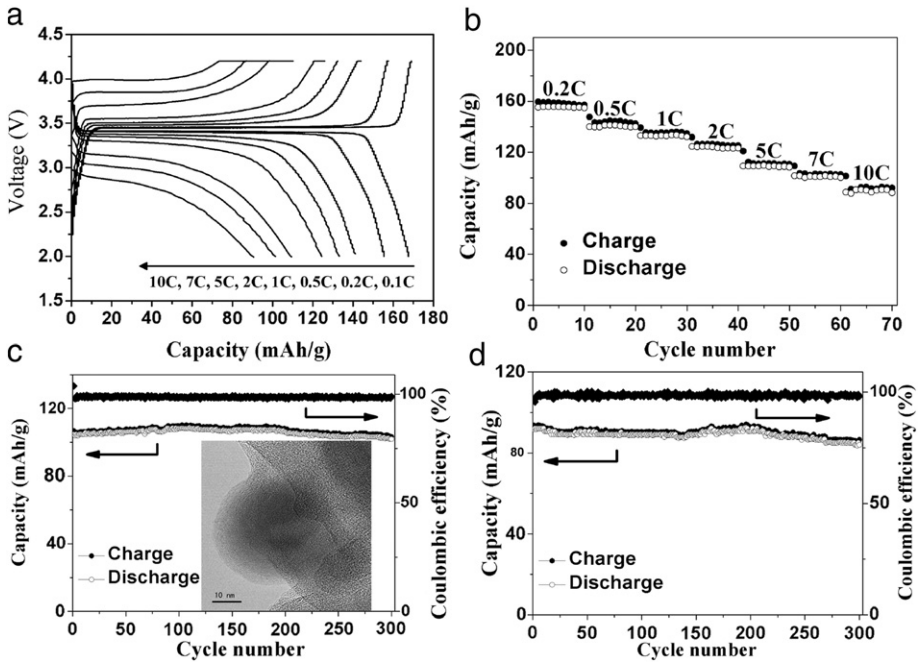

Fig. 3. Electrochemical characterization of GE-LFP: (a) Typical charge/discharge curves and (b) the charge/discharge capacities at different current rates; cycling performance and coulomibic efficiency at (c) 5 and (d) 10 C. The TEM image of GE-LFP after 50 cycles at 5 C was shown in the inset of (c).

4. Conclusions

We successfully synthesized 3D GE-LFP using the GOE-FeOOH as the raw materials. The LFP nanospheres with an average diameter of ~20 nm shorten the lithium ion diffusion length and the intimate contact between LFP nanospheres and graphene makes full use of the graphene's good electronic conductivity to attain a high rate capacity. The excellent high-rate capacities of 108.6 and 90.6 mAh g^{-1} are accomplished and low capacity losses of 2.77% and 8.30% at 5 C and 10 C are achieved.

Acknowledgements

This work is supported by the National Nature Science Foundation of China (No. 51172261) and National Basic Research Program of China (No. 2012CB932300).

References

[1] Lepage D, Michot C, Liang GX, Gauthier M, Schougaard SB. Angew Chem Int Ed 2011;50:6884–7.
[2] Wang Y, Cao G. Adv Mater 2008;20:2251–69.
[3] Toprakci O, Toprakci HAK, Ji L, Xu G, Lin Z, Zhang X. ACS Appl Mater Interfaces 2012;4:1273–80.
[4] Wang YG, Wang YR, Hosono EJ, Wang KX, Zhou HS. Angew Chem Int Ed 2008;47:7461–5.
[5] Dimesso L, Jacke S, Spanheimer C, Jaegermann W. J Alloys Compd 2011;509:3777–82.
[6] Kim HS, Kam DW, Kim WS, Koo HJ. Ionics 2011;17:293–7.
[7] Yi HH, Hu CL, Fang HS, Yang B, Yao YC, Ma WH, et al. Electrochim Acta 2011;56:4052–7.
[8] Yan XB, Chen JT, Yang J, Xue QJ, Miele P. ACS Appl Mater Interfaces 2010;2:2521–9.
[9] Lightcap IV, Kosel TH, Kamat PV. Nano Lett 2010;10:577–83.
[10] Myung S, Solanki A, Kim C, Park J, Kim KS, Lee KB. Adv Mater 2011;23:2221 [-+].
[11] Shi WH, Zhu JX, Sim DH, Tay YY, Lu ZY, Zhang XJ, et al. J Mater Chem 2011;21:3422–7.
[12] Ji LW, Tan ZK, Kuykendall TR, Aloni S, Xun SD, Lin E, et al. Phys Chem Chem Phys 2011;13:7139–46.
[13] Ji LW, Tan ZK, Kuykendall T, An EJ, Fu YB, Battaglia V, et al. Energy Environ Sci 2011;4:3611–6.
[14] Yang SB, Feng XL, Ivanovici S, Mullen K. Angew Chem Int Ed 2010;49:8408–11.
[15] Yang F, Liu Y, Gao L, Sun J. J Phys Chem C 2010;114:22085–91.
[16] Piao YZ, Kim HS, Sung YE, Hyeon T. Chem Commun 2010;46:118–20.
[17] Zhao JQ, He JP, Zhou JH, Guo YX, Wang T, Wu SC, et al. J Phys Chem C 2011;115:2888–94.